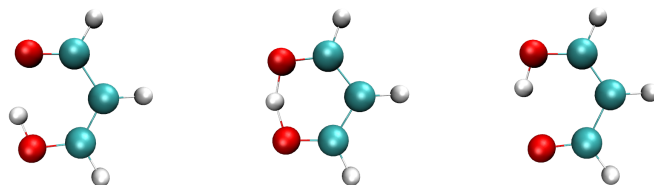




# An RPMD Approach to the Tunnelling Splitting

This thesis was developed in the group of Dr. Stuart C. Althorpe under the supervision of Jeremy O. Richardson during an Erasmus exchange project at the University of Cambridge. The project was carried out under the aegis of Prof. Dr. F. Merkt.



## Abstract

The RPMD method is a very promising way to approximate semiclassical instanton theory computationally. Aim of this thesis is the derivation and application of a numerical formula for the tunnelling splitting in a symmetric double well. In order to do so an analytical, semiclassical expression for a one dimensional tunnelling splitting is derived from instanton theory. This expression, which can be easily generalised to arbitrary dimensions, can be approximated numerically using RPMD-theory. Following this procedure the desired numerical approximation of the tunnelling splitting is obtained. In the second part of this thesis the obtained formula is applied to two interesting special cases: The one dimensional double well and the malonaldehyde-molecule.

Richard Küng

June 2010

# Contents

<b>1</b>	<b>Introduction</b>	<b>3</b>
<b>2</b>	<b>Theory</b>	<b>4</b>
2.1	Tunnelling Splitting . . . . .	4
2.1.1	Degenerate Tunnelling Splitting . . . . .	4
2.1.2	Experimental Evidence . . . . .	6
2.1.3	A Formula for the Tunnelling Splitting . . . . .	6
2.2	Path Integral Formalism . . . . .	7
2.2.1	The Classical Limit . . . . .	8
2.2.2	The Harmonic Approximation . . . . .	8
2.2.3	Calculation of the Partition Functions . . . . .	10
2.3	Result and Finite Dimensional Approach . . . . .	18
2.4	Multidimensional Generalisation . . . . .	22
2.5	RPMD-Theory and the Numerical Algorithm . . . . .	23
2.6	Validity of the approximations . . . . .	25
<b>3</b>	<b>Applications</b>	<b>25</b>
3.1	The One-dimensional Double Well . . . . .	26
3.1.1	Instanton Approach . . . . .	26
3.1.2	Accurate Quantum Mechanical Treatment . . . . .	26
3.1.3	Analytical Semiclassical Result . . . . .	30
3.1.4	Results and Discussion . . . . .	30
3.2	The tunnelling splitting in malonaldehyde . . . . .	33
3.2.1	The considered Potential Energy Surface . . . . .	33
3.2.2	Computational Details . . . . .	34
3.2.3	Results . . . . .	34
3.2.4	Discussion . . . . .	34
<b>4</b>	<b>Conclusion</b>	<b>36</b>

# 1 Introduction

Scientists encountered the effect of quantum mechanical tunnelling for the first time via the radioactive decay in the late 19th century. However it was Friedrich Hund who presented the first mathematical approach for explaining this effect in 1927. In his treatment of enantiomers [1] he proposed that every stationary state of such a system contains the wave functions of both mirror-image-states simultaneously. From this proposition he anticipated a small dispartment in the energy of stationary states in enantiomers. In addition to the essential concept of quantum mechanical tunnelling through a barrier region, Hund’s insights furthermore contain the idea of tunnelling splitting which forms the purpose of this thesis. One year later George Gamow succeeded in providing a mathematical model for the alpha decay of nuclei. Gamow’s insights made Max Born realise that tunnelling is a general aspect of the new (quantum) theory and since then this effect has been a well established aspect of quantum mechanics.

Following R.P Bell [2], this classically impossible phenomenon can be seen to be a consequence of the wave-particle duality. The fact that electromagnetic waves reaching a barrier (e.g. total internal reflection) are not reflected immediately, but rather enter the barrier region with exponentially damped intensity, forms one important result of classical electrodynamics which is often called classical radiation tunnelling. Following de Broglie’s perception that particles have wavelike properties, quantum mechanical tunnelling can be thought to be the material analogon of classical radiation tunnelling.

Tunnelling has a significant impact on many chemical reactions and spectra. One important manifestation is the effect of tunnelling splitting which can influence the spectroscopic data in various molecules. The biggest impact of this effect has been observed in malonaldehyde. This feature makes the intramolecular hydrogen transfer, which is responsible for the extraordinary large tunnelling splitting, in this molecule particularly interesting. Furthermore accurate experimental data for the ground state tunnelling splitting has been published [3] throughout the last years and malonaldehyde therefore has become a very interesting application for quantum chemical studies.

This thesis treats an alternative approach for calculating tunnelling splitting values. It follows the concept of RPMD-theory [4] that has recently yielded very promising results in the determination of quantum mechanical rate constants [5]. Based on path integral formalism, instanton- and RPMD-theory a formula for the tunneling splitting is derived and discussed (section 2). In order to test the validity of this formula it is applied to a one dimensional double well (section 3.1) and to malonaldehyde (section 3.2).

## 2 Theory

### 2.1 Tunnelling Splitting

Tunnelling effects are a well established aspect of quantum mechanics which form a significant factor in many chemical reactions and spectra. The main focus of this thesis lies on the effect of tunnelling splitting which is most relevant for the correct understanding of spectroscopic data.

As R.P. Bell [2] pointed out, degenerate tunnelling (tunnelling between minima that correspond to equivalent structures), usually leads to much bigger effects than nondegenerate tunnelling (tunnelling between minima with different structures) and is therefore in general far more relevant. Thus tunnelling splitting is in most important cases caused by tunnelling between permutation-inversion isomers. The classic example of such an effect is the doubling of lines in the vibrational spectrum of ammonia which was first examined theoretically by Denison and Uhlenbeck [6].

Tunnelling in general strongly depends on the mass of the particle [2, 7] and therefore rather large isotopic effects are to be expected for tunnelling splitting values.

#### 2.1.1 Degenerate Tunnelling Splitting

Degenerate tunnelling splitting refers to a symmetric potential energy surface (PES), because the two minimal energy structures are equivalent. If the two symmetric potential wells are considered to be isolated, each side contains a series of non degenerate energy levels, as illustrated in figure benchmark 1. Let  $E_0$  be the lowest energy state and  $\Psi_0$  the corresponding normalised eigenfunction. For a system that consists of two identical wells, all energy levels become doubly degenerate. However, the barrier is effectively too low and too narrow to consider the two wells as isolated. Therefore it has to be taken into account that  $\Psi_1$  (the ground state wave function of the left well:  $\Psi_0^l$ ) and  $\Psi_2$  (the ground state wave function of the right well:  $\Psi_0^r$ ) perturb each other. Since the unperturbed ground state system is degenerate, degenerate perturbation theory is to be applied [7]. This yields the following eigenfunctions of the perturbed system

$$\begin{aligned}\tilde{\Psi}_1 &= \frac{1}{\sqrt{2}}(\Psi_1 + \Psi_2) \\ \tilde{\Psi}_2 &= \frac{1}{\sqrt{2}}(\Psi_1 - \Psi_2)\end{aligned}$$

The corresponding eigenvalues to  $\tilde{\Psi}_1$  and  $\tilde{\Psi}_2$  can now be calculated

$$\begin{aligned}\tilde{E}_1 &= \langle \tilde{\Psi}_1 | \hat{H} | \tilde{\Psi}_1 \rangle = E_0 + \frac{\Delta}{2} \\ \tilde{E}_2 &= \langle \tilde{\Psi}_2 | \hat{H} | \tilde{\Psi}_2 \rangle = E_0 - \frac{\Delta}{2}\end{aligned}\tag{1}$$

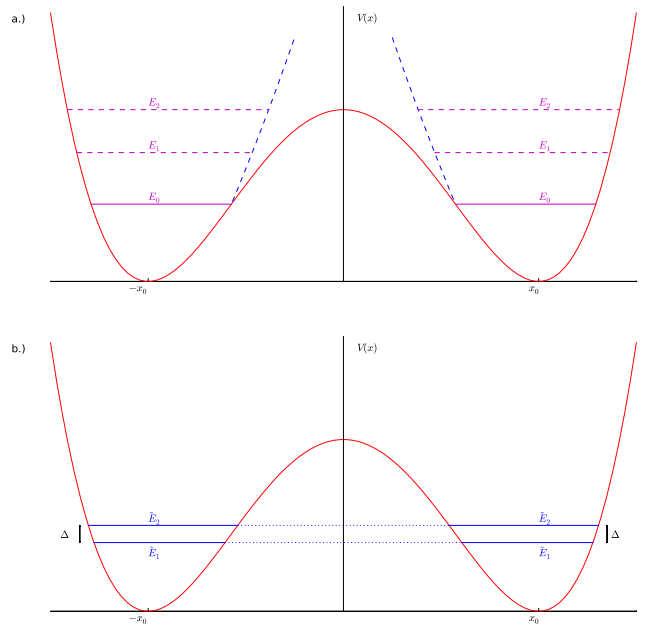


Figure 1: Splitting of the ground state energy level in a double well potential

- a.) If the two wells are considered to be in isolation (here isolation means enlarging the barrier to  $V(x) \rightarrow \infty$  for  $|x| \rightarrow 0$ , as indicated by the dashed blue line), there are a series of discrete energy levels for each well. The symmetry of the wells yields doubly degenerate energy states for the total system.
- b.) In reality the two wells are not in isolation (the barrier is finite) and the eigenfunctions of each well can perturb each other. This leads to an energy splitting of the - in isolation doubly degenerate - zero energy  $E_0$ .

with the tunnelling splitting parameter  $\Delta := 2E_0 \langle \Psi_1 | \Psi_2 \rangle$ . These two energies  $\tilde{E}_1$  and  $\tilde{E}_2$  are not degenerate anymore. One can interpret this result in the following way. Since the two different eigenstates  $\Psi_1$  and  $\Psi_2$  are only separated by a small barrier, they have a non vanishing overlap and can therefore interfere constructively or destructively with each other. Both solutions have to contribute equally to these interference solutions  $\tilde{\Psi}_1$  and  $\tilde{\Psi}_2$  because the PES is symmetric. For the system described by  $\tilde{\Psi}_1$  the probability to be found in the energetically unfavourable barrier region ( $x \approx 0$ ) is larger than for either  $\Psi_1$  or  $\Psi_2$  which leads to a higher energy. With  $\tilde{\Psi}_2$  it is the other way round (e.g.  $P(x=0)dx = \left\| \tilde{\Psi}_2(x=0) \right\|^2 = 0$ ) which yields a lower total energy. Since  $\Delta = 2E_0 \langle \Psi_1 | \Psi_2 \rangle$  and  $\langle \Psi_1 | \Psi_2 \rangle$  is an overlap integral, in principle an approach similar to the LCAO-MO method could be used to determine the tunnelling splitting parameter. Such calculations in general take a long time to be carried out; consequently the LCAO-MO ansatz will not be used in this thesis.

### 2.1.2 Experimental Evidence

The prototype of processes involving tunnelling in a symmetrical double well PES is the inversion of ammonia. In this case the tunnelling effect causes the vibrational levels to be split (thus the name “tunnelling splitting”), where the separation of the doublet is given by  $\Delta$ . Tunnelling splittings can be determined by using various kinds of spectroscopy. In the case of ammonia,  $\Delta$  can be measured experimentally by analysing the vibration-rotation-spectrum of the molecule. For malonaldehyde, accurate values for the tunnelling splitting can be obtained by performing far-infrared [3] and microwave spectroscopy. The fact that accurate experimental data is often available makes various tunnelling splittings a valuable benchmark for theoretical approaches.

### 2.1.3 A Formula for the Tunnelling Splitting

Aim of this section is to derive a formula for the degenerate tunnelling splitting which corresponds to a symmetric potential with two minima separated by a potential barrier. Let us therefore consider a one dimensional system first. The quantum mechanical definition of the partition function yields

$$Q_N = \sum_m e^{-\beta E_m} \quad (2)$$

with  $\beta = \frac{1}{kT}$ , where  $k$  is the Boltzmann constant and  $T$  denotes the Temperature.

In the limit of very low temperatures ( $\beta$  becomes very large), it is sufficient to consider only the first two terms in the whole sum. Thus one can give an approximation to the partition function  $Q_0$  of a system where the tunneling splitting is neglected and an approximation to the partition function  $Q_1$  of a system where the tunneling splitting is taken into account.

$$\begin{aligned}
Q_0 &= 2e^{-\beta E_0} \\
Q_1 &= e^{-\beta(E_0 + \frac{\Delta}{2})} + e^{-\beta(E_0 - \frac{\Delta}{2})} = 2 \cosh\left(\beta \frac{\Delta}{2}\right) e^{-\beta E_0}
\end{aligned}$$

These approximations represent the actual partition functions exactly if the limit  $\beta \rightarrow \infty$  is considered. Applying a Taylor series to the fraction of  $Q_1$  and  $Q_0$  yields

$$\frac{Q_1}{Q_0} = \frac{2 \cosh\left(\beta \frac{\Delta}{2}\right) e^{-\beta E_0}}{2e^{-\beta E_0}} = \cosh\left(\beta \frac{\Delta}{2}\right) = 1 + \frac{1}{2!} \left(\beta \frac{\Delta}{2}\right)^2 + \dots \quad (3)$$

Thus, by calculating the ratio of the partition functions one is able to derive a formula for the tunnelling splitting  $\Delta$ . It is desirable to use a path integral formalism for deriving the partition functions, which shall be discussed in the next chapter.

## 2.2 Path Integral Formalism

The path integral formalism is an alternative description of quantum mechanics without using the concept of operators. It was introduced in 1948 by Feynman and is basically a generalisation of the action principle in classical mechanics [9]. The basic idea of this theory is that for a quantum mechanical system the probability  $P(b, a)$  to go from the point  $x_a$  at the time  $t_a$  to the point  $x_b$  at time  $t_b$  is given by  $P(b, a) = |K(b, a)|^2$ . The ‘‘amplitude’’ (or kernel)  $K(b, a)$  can be found by adding together the contributions of all possible paths that the system could have taken in configuration space to get from  $x_a$  to  $x_b$  in the time  $t_b - t_a$ . The contribution of each path  $x(t)$  is given by  $c e^{i \frac{S}{\hbar}}$ , where  $S = \int_{t_A}^{t_B} \mathcal{L}[x(t)] dt$  denotes the action for the considered trajectory  $x(t)$  (define  $\mathcal{L}[x(t)] := \frac{m}{2} \dot{x}^2 - V(x)$  to be the Lagrangian of the trajectory  $x(t)$ ) and  $c$  denotes a constant that assures that the whole sum converges. Since configuration space is given by a continuum, the continuous limit of this sum has to be taken, and the sum over all paths becomes an integral ( $c \sum_i \rightarrow \int \mathcal{D}x$ ) - the path integral. Thus the formula for the desired probability yields

$$\begin{aligned}
P(b, a) &= |K(b, a)|^2 \\
K(b, a) &= \int e^{i \frac{S[x(t)]}{\hbar}} \mathcal{D}x
\end{aligned}$$

If the time interval  $[t_a, t_b]$  is sliced into  $N$  equidistant pieces  $t_a = t_0 < t_1 < \dots < t_N = t_b$ , the path integral operation can be formally thought to be

$$\begin{aligned}
\int \mathcal{D}x &= \lim_{N \rightarrow \infty} K(N) \int \dots \int dx_1 \dots dx_{N-1} \\
dx_i &= dx(t_i)
\end{aligned}$$

Here  $K(N)$  is a pre-factor that guarantees that the whole expression converges and it is very important to take  $\lim_{N \rightarrow \infty}$  after the actual integration is carried out. A very good introduction to this theory can be found in [9].

### 2.2.1 The Classical Limit

In the path integral formalism all paths contribute equally to the final result, but the phases vary according to their action. For macroscopic systems the action is very big compared to  $\hbar$ , so even for small variations in the path, the phase  $\frac{S}{\hbar}$  varies greatly and small changes in the path generally imply enormous changes in the phase. Therefore the total contribution of neighbouring paths adds to zero, if their action differs from each other. For special paths, namely those which extremise  $S$ , small entanglements in the path lead, at least up to first order, to no change in  $S$ . The contributions of these paths are almost in phase and do not eliminate each other. Only those paths can give substantial contributions to the overall result. In the classical limit ( $\hbar \rightarrow 0$ ) the phases of contributions of neighbouring paths vary so strongly, that only the path that extremises  $S$  contributes to the overall result. Thus the Hamiltonian principle of classical mechanics is obtained.

### 2.2.2 The Harmonic Approximation

Inspired by the implications of the classical limit, one could think of representing every possible path with fixed end points  $x_a = x(t_a)$  and  $x_b = x(t_b)$  as  $x(t) = \tilde{x}(t) + y(t)$ , where  $\tilde{x}(t)$  is the classical trajectory (the minimum action path) and  $y(t)$  denotes the deviation from the classical path ( $y(t) = x(t) - \tilde{x}(t) \forall t \in [t_a, t_b]$ ). Since the initial and final points of all paths are fixed ( $x(t_a) = \tilde{x}(t_a)$  and  $x(t_b) = \tilde{x}(t_b)$ ),  $y(t)$  has to fulfil the boundary condition

$$y(t_a) = y(t_b) = 0 \quad (4)$$

Using the concept of functional derivatives, it is possible to expand the functional  $S[x]$  in  $y$  up to second order. Since  $S[x] = \int_{t_a}^{t_b} \mathcal{L}[x(t)] dt$ , where  $\mathcal{L}[x(t)] = \frac{m}{2} \dot{x}^2 - V(x)$  is the classical Lagrangian of the system, this is equivalent to approximating the potential harmonically ( $V(x) = V(\tilde{x} + y) = V(\tilde{x}) + V'(\tilde{x})y + \frac{1}{2}V''(\tilde{x})y^2$ ). This is the reason why this process is called harmonic approximation.

$$S[x] = S[\tilde{x} + y] = S[\tilde{x}] + \int_{t_a}^{t_b} \frac{\delta S[\tilde{x}]}{\delta \tilde{x}[t]} y(t) dt + \int_{t_a}^{t_b} \int_{t_a}^{t_b} y(t) y(t') \frac{\delta^2 S[\tilde{x}]}{\delta \tilde{x}[t] \delta \tilde{x}[t']} dt dt' + \dots$$

The second term of this expansion yields 0 because  $\frac{\delta S[\tilde{x}(t)]}{\delta \tilde{x}(t)} = 0$  for the minimal action path  $\tilde{x}(t)$ . Using the Euler-Lagrange equation  $\frac{\delta S}{\delta x} = -m\ddot{x} - \frac{dV}{dx}$  from classical mechanics the other term yields

$$\begin{aligned}
\frac{\delta^2 S[\tilde{x}]}{\delta \tilde{x}[t] \delta \tilde{x}[t']} &= \frac{\delta}{\delta \tilde{x}(t')} \left\{ \frac{\delta S[\tilde{x}]}{\delta \tilde{x}} \right\} = \frac{\delta}{\delta \tilde{x}(t')} \left\{ -m\ddot{\tilde{x}} - \frac{dV}{d\tilde{x}} \right\} \\
&= -m \frac{\delta}{\delta \tilde{x}(t')} \ddot{\tilde{x}} - \frac{\delta}{\delta \tilde{x}(t')} \frac{dV}{d\tilde{x}} = -m \frac{d^2}{dt^2} \frac{\delta \tilde{x}(t)}{\delta \tilde{x}(t')} - \frac{d}{d\tilde{x}} \frac{\delta V[\tilde{x}(t)]}{\delta \tilde{x}(t')} \\
&= -m \frac{d^2}{dt^2} \frac{\delta \tilde{x}(t)}{\delta \tilde{x}(t')} - \frac{d}{d\tilde{x}} \frac{dV}{d\tilde{x}} \frac{\delta \tilde{x}(t)}{\delta \tilde{x}(t')} = \left\{ -m \frac{d^2}{dt^2} - \frac{d^2 V}{d\tilde{x}^2} \right\} \delta(t-t')
\end{aligned}$$

where the chain rule  $\frac{\delta V[x(t)]}{\delta x(t')} = \frac{dV}{dx} \frac{\delta x(t)}{\delta x(t')}$  and  $\frac{\delta x(t)}{\delta x(t')} = \delta(t-t')$  were used. By using  $\frac{d\delta(t-t')}{dt} = -\frac{d\delta(t-t')}{dt'}$  (chain rule) and performing twofold integration by parts (the occurring boundary terms vanish because of boundary condition (4)) it can be shown that

$$\begin{aligned}
\int_{t_a}^{t_b} \int_{t_a}^{t_b} y(t) y(t') \frac{\delta^2 S[\tilde{x}]}{\delta \tilde{x}[t] \delta \tilde{x}[t']} dt dt' &= m \int_{t_a}^{t_b} \dot{y}(t)^2 dt - \int_{t_a}^{t_b} \frac{d^2 V}{d\tilde{x}^2} y(t)^2 dt \\
&= m \int_{t_a}^{t_b} y(t) \left\{ -\frac{d^2}{dt^2} - \frac{1}{m} \frac{d^2 V}{d\tilde{x}^2} \right\} y(t) dt
\end{aligned}$$

This yields the formula

$$S[x] = S[\tilde{x}] + S[y] \quad (5)$$

$$S[y] = m \int_{t_a}^{t_b} y(t) \left\{ -\frac{d^2}{dt^2} - \frac{1}{m} \frac{d^2 V}{d\tilde{x}^2} \right\} y(t) dt \quad (6)$$

$\hat{A} := \left\{ -\frac{d^2}{dt^2} - \frac{1}{m} \frac{d^2 V}{d\tilde{x}^2} \right\}$  can be seen as a linear operator operating on the Hilbert-space  $\mathcal{H}$  of curves induced by the scalar product  $\langle a, b \rangle = \int_{t_a}^{t_b} a(t) b(t) dt$ . Since curves essentially are always one dimensional objects, there is no restriction to the actual manifold in which these curves lie. At the moment this manifold is  $\mathbb{R}$  (throughout this thesis the manifold will always be  $\mathbb{R}^n$  for a positive integer  $n$ ). This convenient subtlety (which also implies, that the action  $S[x(t)]$  depends effectively only on one dimension) is the actual reason why the main formula for the tunnelling splitting derived in this section, generalises easily to more than one dimensions. Since  $\hat{A}$  is a linear and self-adjoint operator an orthonormal basis  $\{\phi_i\}_{i \in \mathbb{N}}$  of eigenfunctions of  $\hat{A}$  can be found for  $\mathcal{H}$  which fulfils the following properties:

$$\begin{aligned}
\left\{ -\frac{d^2}{dt^2} - \frac{1}{m} \frac{d^2 V}{d\tilde{x}^2} \right\} \phi_i(t) &= \lambda_i \phi_i(t) \\
\int_{t_a}^{t_b} \phi_i(t) \phi_j(t) dt &= \delta_{ij} \quad \forall i, j \in \mathbb{N}
\end{aligned}$$

Since  $y(t) \in \mathcal{H}$  one is thus able to write

$$y(t) = \sum_i \nu_i \phi_i(t)$$

Therefore

$$\begin{aligned} S[y] &= m \int_{t_a}^{t_b} y(t) \left\{ -\frac{d^2}{dt^2} - \frac{1}{m} \frac{d^2 V}{d\tilde{x}^2} \right\} y(t) dt = m \int_{t_a}^{t_b} y(t) \hat{A} y(t) dt \\ &= m \int_{t_a}^{t_b} \sum_i \nu_i \phi_i(t) \hat{A} \sum_j \nu_j \phi_j(t) dt = m \sum_{ij} \nu_i \nu_j \int_{t_a}^{t_b} \phi_i(t) \hat{A} \phi_j(t) dt \\ &= m \sum_{ij} \lambda_j \nu_i \nu_j \int_{t_a}^{t_b} \phi_i(t) \phi_j(t) dt = m \sum_i \lambda_i \nu_i^2 \end{aligned}$$

Which yields the following formula for the harmonic approximation:

$$S[x] = S[\tilde{x}] + m \sum_i \lambda_i \nu_i^2 \quad (7)$$

The harmonic approximation yields good results for the following cases:

1. *A quadratic potential:* Here the action is quadratic as well and the expansion up to second order describes the actual action exactly. The harmonic approximation in this case already yields the exact result.
2. *The semiclassical regime:* As a rule of thumb [9] trajectories other than  $\tilde{x}$  (the classical trajectory) only contribute to the total result as long as the action is still within about  $\hbar$  of  $S[\tilde{x}]$ . If  $\frac{S[\tilde{x}]}{\hbar}$  therefore is already “rather” big, it is likely that quite small variations of  $\tilde{x}$  already lead to changes in the action of about  $\hbar$ . In this case one can see the harmonic approximation as considering only small variations of  $\tilde{x}$  (up to second order in  $y$ ), rather than approximating the potential harmonically.
3. *As harmonic approximation to the potential around a minimum.*
4. *Considering a short time interval:* A particle moving along a path very different from the classical trajectory needs to have a large extra velocity to make this larger route in time (it has to get to the fixed end point  $x_b$  within the fixed time  $t_b - t_a$ ). This yields an extra large kinetic energy ( $T[x(t)] = \frac{m}{2} \dot{x}(t)^2$ ) which greatly amplifies the action ( $S = \int_{t_a}^{t_b} \{T[x(t)] - V[x(t)]\} dt$ ). Thus the action will be very large for such paths and the contributions of neighbouring paths will (like in the classical limit) add up to zero.

### 2.2.3 Calculation of the Partition Functions

All in all the path integral, as it was introduced above, is nothing but the representation of a quantum mechanical propagator  $K(b, a) := K(x_b, x_a, t_b - t_a)$ .

For a system  $x_a$  to turn into system  $x_b$  after the time  $t_b - t_a$  the propagator can be written as

$$K(b, a) = \int_{x(t_a)=x_a}^{x(t_b)=x_b} e^{i \frac{S[x(t)]}{\hbar}} \mathcal{D}x$$

Where the notation  $\int_{x(t_a)=x_a}^{x(t_b)=x_b}$  clarifies that only paths that fulfil  $x(t_a) = x_a$  and  $x(t_b) = x_b$  need to be considered. In conventional quantum mechanics the same propagator can be written in terms of the energy eigenfunctions  $\Psi_k$  with eigenvalues  $E_k^0$

$$K(b, a) = \sum_k \exp \left\{ -\frac{i}{\hbar} E_k^0 (t_b - t_a) \right\} \langle x_b | \Psi_k \rangle \langle \Psi_k | x_a \rangle \quad (8)$$

Formula (8) is already very similar to the density matrix of the same system, because the Boltzmann operator in terms of  $\Psi_k$  yields

$$e^{-\beta \hat{H}} = \sum_k \exp \{ -\beta E_k^0 \} | \Psi_k \rangle \langle \Psi_k |$$

and therefore the density matrix  $\rho(b, a)$  can be written as

$$\rho(b, a) = \langle x_b | e^{-\beta \hat{H}} | x_a \rangle = \sum_k \exp \{ -\beta E_k^0 \} \langle x_b | \Psi_k \rangle \langle \Psi_k | x_a \rangle \quad (9)$$

In fact formula (9) - and therefore  $\rho(b, a)$  - can be obtained by formally replacing  $i(t_b - t_a)$  by  $\hbar\beta$  in formula (8). This change of variables is called a Wick rotation ( $t \rightarrow i\tau$ ,  $x \rightarrow x$ ,  $\dot{x} \rightarrow i\dot{x}$ ,  $V(x) \rightarrow -V(x)$ ) and transforms the system from Minkowski space ( $ds^2 = -dt^2 + dx^2 + dy^2 + dz^2$ ) to Euclidian space ( $ds^2 = d\tau^2 + dx^2 + dy^2 + dz^2$ ). Due to this rotation the potential changes its sign and the Lagrangian  $\mathcal{L} = \frac{1}{2}\dot{x}^2 - V(x)$  is replaced by the classical Hamiltonian  $H = \frac{1}{2}\dot{x}^2 + V(x)$ . The resulting Euclidian action  $S_E = \int_0^{\hbar\beta} H[x(\tau)] d\tau$  with  $\beta = \frac{1}{\hbar T}$  therefore describes the conventional action along an upside down potential. The quantum mechanical partition function is formally given by

$$Q(T) = \text{tr} \left[ e^{-\beta \hat{H}} \right]$$

where  $\text{tr} [\hat{A}]$  denotes the trace of an arbitrary operator  $\hat{A}$  ( $\text{tr} [\hat{A}] := \sum_i \langle \Psi_i | \hat{A} | \Psi_i \rangle$ ) for an arbitrary orthonormal basis  $\{ \Psi_i \}_{i \in \mathbb{N}}$ . Thus by using formula (9) and the Wick-rotated formula (8) a path integral expression for  $Q(T)$  can be obtained.

$$\begin{aligned} Q(T) &= \text{Tr} \left[ e^{-\beta \hat{H}} \right] = \int \langle x | e^{-\beta \hat{H}} | x \rangle dx = \int \sum_k \exp \{ -\beta E_k^0 \} \langle x | \Psi_k \rangle \langle \Psi_k | x \rangle dx \\ &= \int K_E(x, x, \hbar\beta) dx = \int \left\{ \int_{x(0)=x}^{x(\hbar\beta)=x} e^{-\frac{S_E[x(t)]}{\hbar}} \mathcal{D}x \right\} dx \end{aligned}$$

where  $K_E(x, x, \hbar\beta)$  denotes the Wick-rotated Euclidian propagator. Since every considered path begins and ends in  $x$  this yields the following expression

$$Q = \int \left\{ \int_{x(0)=x(\hbar\beta)} e^{-\frac{1}{\hbar} S_E[x]} \mathcal{D}x \right\} dx(0) \quad (10)$$

where  $\int_{x(0)=x(\hbar\beta)} \mathcal{D}x$  denotes the (according to path integral theory) correct summation (integration) over all closed paths that begin and end in  $x(0)$ .  $\int dx(0)$  indicates the summation over all possible initial (and final) points of the paths considered in  $\int_{x(0)=x(\hbar\beta)} \mathcal{D}x$ . In general  $x(0)$  can be an arbitrary point of the overall manifold (in this case  $\mathbb{R}$ ) which consists of a continuum rather than of discrete values. To take this into account one has to take the continuous limit in which the sum becomes an integral. One can now apply the harmonic approximation to this formula. As discussed above only variations  $y$  around classical trajectories  $\tilde{x}$  - or better: trajectories that fulfill  $\frac{\delta S[x(t)]}{\delta x(t)} = 0$  - are considered. Since only closed paths are taken into account and the initial (and thus final) points of the  $y$ -variations are furthermore fixed, the only initial points  $x(0)$  that need to be considered are the classical ones  $\tilde{x}(0)$ . Therefore  $\int dx(0)$  can be reduced to  $\int d\tilde{x}(0)$ . In all cases relevant to this thesis the number of different  $\tilde{x}$  is finite. Therefore  $\int d\tilde{x}(0)$ , which describes the sum over all possible starting points, can be reduced to an actual sum - in short:  $\int dx(0) \longrightarrow \int d\tilde{x}(0) \longrightarrow \sum_{\text{different } \tilde{x}}$ . Furthermore

$$\begin{aligned} \int_{x(0)=x(\hbar\beta)} e^{-\frac{1}{\hbar} S_E[x]} \mathcal{D}x &= \int_{y(0)=y(\hbar\beta)=0} e^{-\frac{1}{\hbar} (S_E[\tilde{x}] + S_E[y])} \mathcal{D}y \\ &= e^{-\frac{1}{\hbar} S_E[\tilde{x}]} \int_{y(0)=y(\hbar\beta)=0} e^{-\frac{1}{\hbar} S_E[y]} \mathcal{D}y \end{aligned}$$

since  $\mathcal{D}x = \mathcal{D}(\tilde{x} + y) = \mathcal{D}y$  because  $\tilde{x}$  is fixed throughout the whole integration and only closed variations with  $y(0) = y(\hbar\beta) = 0$  have to be taken into account. Formula (10) is therefore reduced to

$$Q = \sum_{\text{different } \tilde{x}} e^{-\frac{1}{\hbar} S_E[\tilde{x}]} \int_{y(0)=y(\hbar\beta)=0} e^{-\frac{1}{\hbar} S_E[y]} \mathcal{D}y \quad (11)$$

**Calculation of  $Q_0$**  In this case tunnelling effects are neglected and one is able to restrain the problem to one side of the symmetric potential and disregard any possible effect that might come from the other side. In this case the only classical trajectory  $\tilde{x}$  (the path that minimises the action) of a particle in the ground state is a constant trajectory  $\tilde{x} = -x_0$  (or  $\tilde{x} = x_0$  respectively) which simply corresponds to a classical particle resting in the minimum. This trajectory is really the only one that extremises  $S_E$  because it corresponds to the maximum of the upside-down potential that has to be considered in  $S_E$ . The Euclidian action of such a path simply yields  $S_E[\tilde{x}] = \int_0^{\hbar\beta} \left( \frac{m}{2} \dot{\tilde{x}}^2 + V(\tilde{x}) \right) d\tau = V_0 \int_0^{\hbar\beta} d\tau$ ,

where  $V_0$  is the potential energy at the minimum. Since the potential is only defined up to a constant,  $V_0$  can be without loss of generality set to zero which leads to  $S_E[\tilde{x}] = 0$ . With the harmonic approximation  $V(x) = \frac{1}{2}m\omega^2x^2$  and taking into account that because of the Wick rotation the upside down potential has to be considered in formula (10), one obtains for  $S_E[y]$ :

$$\begin{aligned} S_E[y] &= \int_0^{\hbar\beta} y(\tau) \left\{ -m \frac{d^2}{d\tau^2} + \frac{d^2V}{dx^2} \right\} y(\tau) d\tau = m \int_0^{\hbar\beta} y(\tau) \left\{ -\frac{d^2}{d\tau^2} + \omega^2 \right\} y(\tau) d\tau \\ &= m \sum_i \lambda_i \nu_i^2 \end{aligned}$$

If one takes a closer look at the operator  $\left\{ -\frac{d^2}{d\tau^2} + \omega^2 \right\}$  and considers the restraining condition (4) ( $y(0) = y(\hbar\beta) = 0$ ), which has to hold for every relevant path  $y(t)$ , the Hamiltonian (modified by an additional constant  $\omega^2$ ) and the boundary condition are exactly the same, as for the one dimensional particle in a box. Thus the eigenfunctions and eigenvalues are

$$\begin{aligned} \nu_i(\tau) &= \sqrt{\frac{2}{\hbar\beta}} \sin(\omega_i\tau) \\ \lambda_i &= \omega_i^2 + \omega^2 \\ \omega_i &= \frac{2\pi i}{\hbar\beta} \end{aligned} \tag{12}$$

It is very important to mention that formula (12) is only valid for continuous functions and has to be altered when finite dimensional (and thus non-continuous) approximations are used. Using formula (11) one can now calculate the partition function

$$\begin{aligned} Q_o &= \sum_{\text{different } \tilde{x}} e^{-\frac{1}{\hbar}S_E[\tilde{x}]} \int_{y(0)=y(\hbar\beta)=0} e^{-\frac{1}{\hbar}S_E[y]} \mathcal{D}y \\ &= 2e^{-\frac{S_E[\tilde{x}]}{\hbar}} \int_{y(0)=y(\hbar\beta)=0} e^{-\frac{m}{\hbar} \sum_i (\omega_i^2 + \omega^2) \nu_i^2} \mathcal{D}y \\ &= 2 \lim_{N \rightarrow \infty} K(N) \int \dots \int e^{-\frac{m}{\hbar} \sum_{i=1}^N (\omega_i^2 + \omega^2) \nu_i^2} dy(\tau_1) \dots dy(\tau_{N-1}) \\ &= 2 \lim_{N \rightarrow \infty} K(N) \int \dots \int e^{-\frac{m}{\hbar} \sum_{i=1}^N (\omega_i^2 + \omega^2) \nu_i^2} d\nu_1 \dots d\nu_{N-1} \end{aligned}$$

It is important that the limit  $N \rightarrow \infty$  is carried out after performing the integration. Thus it can be assumed that  $y_1 \dots y_N$  (which can be thought as the canonical basis of an  $N$ -dimensional vector space) and  $\nu_1 \dots \nu_N$  are a finite set of vectors and the operator can be therefore represented by a finite dimensional hermitian matrix. Since  $\nu_1 \dots \nu_N$  form the eigenbasis of that hermitian

matrix it can be without loss of generality assumed that this is an orthonormal basis of the considered vector space. Thus the mapping  $T : y \rightarrow \nu$  is a linear, orthogonal transformation and can be represented by an orthogonal transformation matrix  $T_{N \times N}$ . This implies  $|\det(T_{N \times N})| = 1$  which yields the transformation  $\int \dots \int dy_1 \dots dy_{N-1} \rightarrow \int \dots \int d\nu_1 \dots d\nu_{N-1}$  used above. The fact that the integration over  $y_N$ , and  $\nu_N$  respectively, is omitted has no impact on the result because finally the limit  $N \rightarrow \infty$  is considered. The whole procedure yields the following expression

$$Q_0 = 2 \lim_{N \rightarrow \infty} K(N) \prod_{i=1}^N \sqrt{\frac{2\pi\hbar}{m(\omega_i^2 + \omega^2)}} \quad (13)$$

**Calculation of  $Q_1$**  In this case tunneling effects are not neglected anymore, therefore the total potential has to be considered and there do exist more paths  $\tilde{x}$  that yield  $\frac{\delta S_E[\tilde{x}]}{\delta \tilde{x}} = 0$ . The first two paths are the constant paths  $\tilde{x}(\tau) = \pm x_0$  - the particle stays in either minimum without movement. The result for both of them is therefore  $Q_0$  again. A third solution is a  $\hbar\beta$  periodic upside-down barrier trajectory  $x_{ins}$ , that is called instanton [8].  $x_{ins}$  is not a minimum of the action, but rather a saddle point.  $x_{ins}$  however changes its character in the limit  $\hbar\beta \rightarrow \infty$  and turns into a minimum which is very useful when it comes to approximating it numerically. Furthermore  $x_{ins}$  is only different from a constant path if  $\beta$  exceeds some  $\beta_{cross}$  which depends on the PES. If one considers the  $\lim \hbar\beta \rightarrow \infty$  the instanton stays an infinite amount of time in the vicinity of the first minimum, crosses the (upside down) barrier during some finite time, stays in the vicinity of the second minimum for another infinite amount of time and crosses the (upside down) barrier region during some finite time again to get back to its starting position. Apart from these three paths there are more trajectories with  $\frac{\delta S_E[\tilde{x}]}{\delta \tilde{x}} = 0$ . They correspond to multiple crossings of the barrier region. One could show that these trajectories correspond to higher terms in the Taylor approximation of  $\cosh\left(\frac{\beta\hbar}{2}\right)$ , but this would go beyond the scope of this thesis. For small variations around  $x_{ins}$  the action up to first order nevertheless doesn't change and the vicinity of that path therefore also contributes to the overall path integral. Therefore

$$Q_1 = 2Q_0 + Q_{ins} + \dots$$

Under the assumption of the harmonic approximation one is able to calculate  $Q_{ins}$  in a similar way as  $Q_0$  was calculated.

$$\begin{aligned} Q_{ins} &= \int e^{-\frac{1}{\hbar} S_E[x]} \mathcal{D}x \\ S_E[x] &= S_E[x_{ins}] + S_E[y] \\ S_E[y] &= m \int_0^{\hbar\beta} y(\tau) \left\{ -\frac{d^2}{d\tau^2} + \frac{1}{m} \frac{d^2 V}{dx^2} \right\} y(\tau) d\tau = m \sum \eta_i \nu_i^2 \end{aligned}$$

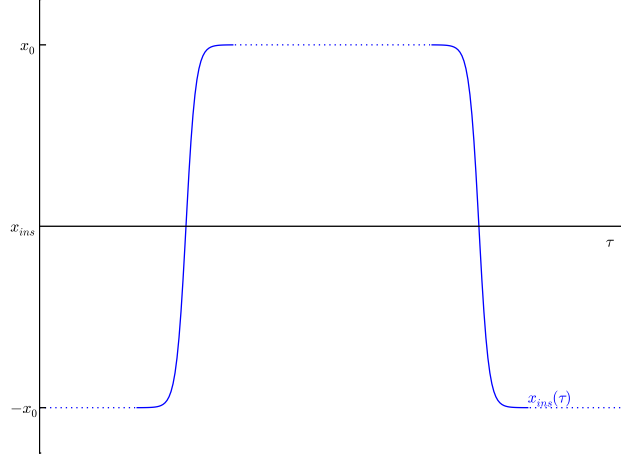


Figure 2: Sketch of an ideal instanton trajectory  $x_{inst}(\tau)$ . The dashed lines depict infinitely long straight lines.

where  $\eta_i$  are the eigenvalues and  $\nu_i$  denote the eigenfunctions of the operator  $\left\{-\frac{d^2}{d\tau^2} + \frac{1}{m} \frac{d^2 V}{dx^2}\right\}$ . Actually two of the eigenvalues - without loss of generality  $\eta_1$  and  $\eta_2$  - are zero. One way of showing this is to first look at the function  $\nu_1 := N\dot{x}_{inst}$ , where  $N$  is a normalisation constant that guarantees  $\langle \nu_1, \nu_1 \rangle = 1$ . Namely

$$\begin{aligned} \langle \nu_1, \nu_1 \rangle &= N^2 \int_0^{\hbar\beta} \dot{x}_{inst}^2 d\tau = 1 \\ N &= (S_0)^{-\frac{1}{2}} \\ S_0 &:= \int_0^{\hbar\beta} \dot{x}_{inst}^2 d\tau \end{aligned}$$

$$\begin{aligned}
\left\{-\frac{d^2}{d\tau^2} + \frac{1}{m} \frac{d^2V}{dx^2}\right\} \nu_1 &= \frac{N}{m} \left\{-m \frac{d^2}{d\tau^2} \dot{x}_{ins} + \frac{d^2V}{dx^2} \dot{x}_{ins}\right\} \\
&= \frac{N}{m} \left\{-m \frac{d^3}{d\tau^3} x_{ins} + \frac{d}{dx} \frac{dV[x_{ins}(\tau)]}{dx} \frac{d}{d\tau} x_{ins}(\tau)\right\} \\
&= \frac{N}{m} \left\{-m \frac{d^3}{d\tau^3} x_{ins} + \frac{d}{dx} \frac{dV[x_{ins}(\tau)]}{d\tau}\right\} \\
&= \frac{N}{m} \frac{d}{d\tau} \left\{-m \frac{d^2}{d\tau^2} x_{ins} + \frac{d}{dx} V[x_{ins}]\right\} \\
&= \frac{N}{m} \frac{d}{d\tau} \left\{\frac{\delta S_E[x_{ins}]}{\delta x_{ins}}\right\} = 0
\end{aligned}$$

where the chain rule, the Euler Lagrange equation ( $\frac{\delta S_E}{\delta x} = -m\ddot{x} + \frac{dV}{dx}$ ) and the fact that the instanton trajectory is a saddle point of the action ( $\frac{\delta S_E[x_{ins}]}{\delta x_{ins}} = 0$ ) were used. Obviously  $\nu_1$  is a non trivial eigenfunction with eigenvalue 0. To find  $\nu_2$  it is necessary to consider the limit  $\hbar\beta \rightarrow \infty$ . In this case, as already mentioned above, an infinite amount of time separates the two parts of the instanton trajectory that include the actual movement (going from one minimum to the other - kink; and going back again - antikink). It is therefore possible to fix a certain time  $a$  that is separated from both kink and antikink by an infinite amount of time. One is now able to construct the following function:

$$\nu_2(\tau) = \begin{cases} +N\dot{x}_{ins} & 0 \leq \tau < a \\ -N\dot{x}_{ins} & a < \tau \\ 0 & a = \tau \end{cases}$$

with  $N$  defined exactly as above. This function is smooth in  $\lim \hbar\beta \rightarrow \infty$ , quadratic integrable and it fulfills  $\left\{-\frac{d^2}{d\tau^2} + \frac{1}{m} \frac{d^2V}{dx^2}\right\} \nu_2 = 0$ .  $\nu_2$  is furthermore linearly independent from  $\nu_1$  and therefore provides a second zero eigenvalue in the spectrum of  $\left\{-\frac{d^2}{d\tau^2} + \frac{1}{m} \frac{d^2V}{dx^2}\right\}$ . Due to the normalisation condition one is able to substitute and carry out the following integration for  $i = 1, 2$

$$\int d\nu_i = \int_0^{\hbar\beta} \sqrt{S_0} d\tau = \sqrt{S_0} \int_0^{\hbar\beta} d\tau = \hbar\beta \sqrt{S_0}$$

Now  $Q_{ins}$  can be calculated:

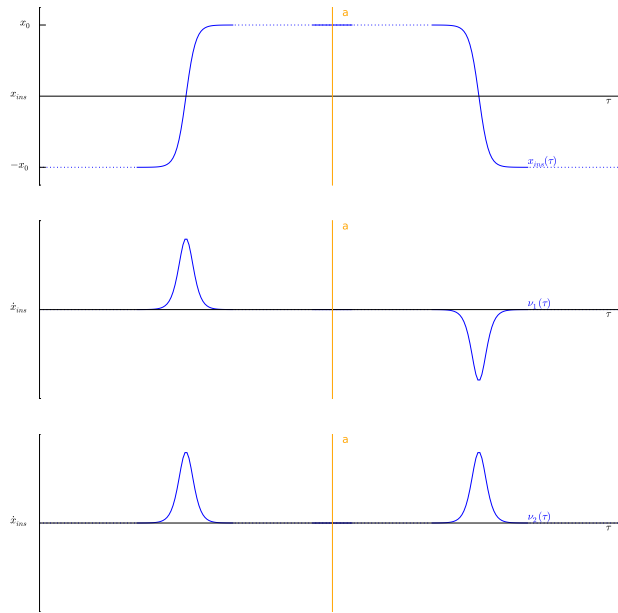


Figure 3: Sketch of  $x_{ins}$  and the eigenfunctions  $\nu_1$  and  $\nu_2$

$$\begin{aligned}
Q_{ins} &= e^{-\frac{S_E[x_{ins}]}{\hbar}} \int_{y(0)=y(\hbar\beta)=0} e^{-\frac{1}{\hbar}S_E[y]} \mathcal{D}y = e^{-\frac{S_E[x_{ins}]}{\hbar}} \int e^{-\frac{m}{\hbar} \sum_i \eta_i \nu_i^2} \mathcal{D}y \\
&= e^{-\frac{S_E[x_{ins}]}{\hbar}} \lim_{N \rightarrow \infty} K(N) \int \cdots \int e^{-\frac{m}{\hbar} \sum_{i=1}^N \eta_i \nu_i^2} dy(\tau_1) \cdots dy(\tau_{N-1}) \\
&= e^{-\frac{S_E[x_{ins}]}{\hbar}} \int d\nu_1 \int d\nu_2 \lim_{N \rightarrow \infty} K(N) \prod_{i=3}^N \int e^{-\frac{m}{\hbar} \eta_i \nu_i^2} d\nu_i \\
&= e^{-\frac{S_E[x_{ins}]}{\hbar}} \left( \hbar\beta\sqrt{S_0} \right)^2 \lim_{N \rightarrow \infty} K(N) \prod_{i=3}^N \sqrt{\frac{2\pi\hbar}{m\eta_i}}
\end{aligned}$$

The substitution  $\int \cdots \int dy(\tau_1) \cdots dy(\tau_{N-1}) \rightarrow \int \cdots \int d\nu_1 \cdots d\nu_{N-1}$  can be carried out completely analogous to the previous section. This yields the following expression for  $Q_1$  :

$$Q_1 = 2Q_0 + e^{-\frac{S_E[x_{ins}]}{\hbar}} \hbar^2 \beta^2 S_0 \lim_{N \rightarrow \infty} K(N) \prod_{i=3}^N \sqrt{\frac{2\pi\hbar}{m\eta_i}} + \dots \quad (14)$$

### 2.3 Result and Finite Dimensional Approach

Combining the main results from section 1.2

$$\begin{aligned}
Q_0 &= 2 \lim_{N \rightarrow \infty} K(N) \prod_{i=1}^N \sqrt{\frac{2\pi\hbar}{m(\omega_i^2 + \omega^2)}} \\
Q_1 &= 2Q_0 + e^{-\frac{S_E[x_{ins}]}{\hbar}} \hbar^2 \beta^2 S_0 \lim_{N \rightarrow \infty} K(N) \prod_{i=3}^N \sqrt{\frac{2\pi\hbar}{m\eta_i}} + \dots
\end{aligned}$$

and writing  $S_{ins} := S_E[x_{ins}]$ , one obtains the following expression for  $\frac{Q_1}{Q_0}$  :

$$\begin{aligned}
\frac{Q_1}{Q_0} &= 1 + \frac{e^{-\frac{S_{ins}}{\hbar}} \hbar^2 \beta^2 S_0 \lim_{N \rightarrow \infty} K(N) \prod_{i=3}^N \sqrt{\frac{2\pi\hbar}{m\eta_i}}}{2 \lim_{N \rightarrow \infty} K(N) \prod_{i=1}^N \sqrt{\frac{2\pi\hbar}{m(\omega_i^2 + \omega^2)}}} + \dots \\
&= 1 + \frac{m\hbar^2 \beta^2 S_0 \prod_{i=1}^{\infty} \sqrt{\omega_i^2 + \omega^2}}{4\pi\hbar \prod_{i=3}^{\infty} \sqrt{\eta_i}} e^{-\frac{S_{ins}}{\hbar}} + \dots
\end{aligned}$$

This expression can now be combined with equation (3)

$$\frac{Q_1}{Q_0} = \frac{2 \cosh\left(\beta \frac{\Delta}{2}\right) e}{2e^{-\beta E_0}} = \cosh\left(\beta \frac{\Delta}{2}\right) = 1 + \frac{1}{2} \left(\beta \frac{\Delta}{2}\right)^2 + \dots$$

to obtain the desired expression for the tunnelling splitting  $\frac{\Delta}{2}$  which is exact in the lim  $\hbar\beta \rightarrow \infty$

$$\frac{\Delta}{2} = \left( \frac{m\hbar S_0 \prod_{i=1}^{\infty} \sqrt{\omega_i^2 + \omega^2}}{4\pi \prod_{i=3}^{\infty} \sqrt{\eta_i}} \right)^{\frac{1}{2}} e^{-\frac{S_{ins}}{2\hbar}} \quad (15)$$

**Finite Dimensional Approach** In the finite dimensional approach the (imaginary) time interval  $[0, \hbar\beta]$  is approximated by an equidistant finite number of  $N$  time steps  $0 = \tau_0 < \tau_1 < \dots < \tau_N = \hbar\beta$ . The instanton trajectory  $x_{ins}$  is therefore represented by a finite number of points  $x_i := x_{ins}(\tau_i)$ . This leads to a finite dimensional approximation to the expressions occurring in (15). Using the Riemann sum approximation for integrals ( $\int_a^b f(x) dx \approx \frac{b-a}{N} \sum_{i=1}^N f(x_i)$  for sufficiently large  $N$ ) and the finite dimensional approach to derivatives ( $\frac{d}{dx} f(x) \approx \frac{f(x+h) - f(x)}{h}$  for sufficiently small  $h$ ), one can obtain a finite dimensional approach to all expressions used in formula (15)

$$\begin{aligned} H[x_i] &= \frac{m}{2} \dot{x}_i^2 + V(x_i) \approx \frac{m}{2} \left( \frac{x_{i+1} - x_i}{\frac{\hbar\beta}{N}} \right)^2 + V(x_i) \\ &= V(x_i) + \frac{m}{2 \left(\frac{\beta}{N}\hbar\right)^2} (x_{i+1} - x_i)^2 \\ S_{ins} &= \int_0^{\hbar\beta} H[x_{ins}(\tau)] d\tau \approx \frac{\hbar\beta}{N} \sum_{i=1}^N H[x_i] \\ &\approx \hbar \frac{\beta}{N} \sum_{i=1}^N \left( V(x_i) + \frac{m}{2 \left(\frac{\beta}{N}\hbar\right)^2} (x_{i+1} - x_i)^2 \right) \\ S_0 &= \int_0^{\hbar\beta} \dot{x}_{ins}^2(\tau) d\tau \approx \frac{\hbar\beta}{N} \sum_{i=1}^N \dot{x}_{ins}^2(\tau_i) \\ &\approx \frac{\hbar\beta}{N} \sum_{i=1}^N \left( \frac{x_{ins}(\tau_{i+1}) - x_{ins}(\tau_i)}{\frac{\beta}{N}} \right)^2 = \frac{N}{\hbar\beta} \sum_{i=1}^N (x_{i+1} - x_i)^2 \end{aligned}$$

Applying the definitions for the instanton trajectory  $\tilde{x} := x_{ins}$

$$\begin{aligned}\beta_N &:= \frac{\beta}{N} \\ \tilde{U}_N &:= \sum_{i=1}^N \left( V(\tilde{x}_i) + \frac{m}{2(\beta_N \hbar)^2} (\tilde{x}_{i+1} - \tilde{x}_i)^2 \right) \\ B_N &:= \sum_{i=1}^N (\tilde{x}_{i+1} - \tilde{x}_i)^2\end{aligned}\tag{16}$$

the approximations above reduce to  $S_{ins} \approx \hbar \beta_N \tilde{U}_N$  as well as  $S_0 \approx \frac{1}{\hbar \beta_N} B_N$  and formula (15) becomes

$$\begin{aligned}\frac{\Delta}{2} &= \left( \frac{m \hbar S_0}{4\pi} \frac{\prod_{i=1}^{\infty} \sqrt{\omega_i^2 + \omega^2}}{\prod_{i=3}^{\infty} \sqrt{\eta_i}} \right)^{\frac{1}{2}} e^{-\frac{S_{ins}}{2\hbar}} \approx \left( \frac{m \hbar B_N}{4\pi \hbar \beta_N} \frac{\prod_{i=1}^N \sqrt{\omega_i^2 + \omega^2}}{\prod_{i=3}^N \sqrt{\eta_i}} \right)^{\frac{1}{2}} e^{-\frac{1}{2\hbar} \hbar \beta_N \tilde{U}_N} \\ &= \left( \frac{m B_N}{4\pi \beta_N} \frac{1}{(\beta_N \hbar)^2} \frac{\prod_{i=1}^N \beta_N \hbar \sqrt{\omega_i^2 + \omega^2}}{\prod_{i=3}^N \beta_N \hbar \sqrt{\eta_i}} \right)^{\frac{1}{2}} e^{-\frac{1}{2} \beta_N \tilde{U}_N}\end{aligned}$$

Therefore the finite dimensional approximation to the tunnelling splitting  $\frac{\Delta}{2}$  is described by

$$\frac{\Delta}{2} = \frac{1}{\beta_N \hbar} \left( \frac{m B_N}{4\pi \beta_N} \frac{\prod_{i=1}^N \beta_N \hbar \sqrt{\omega_i^2 + \omega^2}}{\prod_{i=3}^N \beta_N \hbar \sqrt{\eta_i}} \right)^{\frac{1}{2}} e^{-\frac{1}{2} \beta_N \tilde{U}_N}\tag{17}$$

As already mentioned above, formula (12) ( $\omega_i = \frac{2\pi i}{\beta \hbar}$ ) is only valid for continuous functions. The finite dimensional approximation used above however does not fulfil this strict condition and formula (12) therefore has to be altered. If  $N$  depicts the fineness introduced above, the operator  $-\frac{d^2}{di^2}$  (with  $y_i := y(\tau_i)$ ) and the boundary condition  $y_1 = y_{N+1} = 0$  which follows from the boundary

condition (4) can be represented by a  $N \times N$ -matrix  $\mathbf{A}$

$$\begin{aligned} -\frac{d^2}{dt^2}y &\approx -\frac{\dot{y}_{i+1} - \dot{y}_i}{\beta_N \hbar} \approx -\frac{(y_{i+1} - y_i) - (y_i - y_{i-1})}{(\beta_N \hbar)^2} \\ &= \begin{pmatrix} \gamma & \delta & 0 & \dots & 0 & \delta \\ \delta & \gamma & \delta & & & 0 \\ 0 & \delta & \ddots & \ddots & & \vdots \\ \vdots & & \ddots & \ddots & \delta & 0 \\ 0 & & & \delta & \gamma & \delta \\ \delta & 0 & \dots & 0 & \delta & \gamma \end{pmatrix} \begin{pmatrix} y_1 \\ \vdots \\ \vdots \\ y_N \end{pmatrix} \end{aligned}$$

with  $\gamma := \frac{2}{(\beta_N \hbar)^2}$  and  $\delta := -\frac{1}{(\beta_N \hbar)^2}$  (this notation makes the link to Hueckel theory obvious). In order to simplify the mathematics of this problem it is useful to replace the boundary condition  $y_1 = y_{N+1} = 0$  by the weaker demand  $y_1 = y_{N+1}$  that contains the former as a special case. Because of this periodic boundary condition the eigenfunctions of that matrix can be guessed to be:

$$\begin{aligned} \phi_j &= (\phi_j^1, \dots, \phi_j^N)^T \\ \phi_j^k &= \exp\left\{\frac{2\pi i}{N}jk\right\} \end{aligned}$$

This yields for the  $k$ -th component of  $\mathbf{A}\phi_j$ :

$$\begin{aligned} (\mathbf{A}\phi_j)^k &= \delta\phi_j^{k-1} + \gamma\phi_j^k + \delta\phi_j^{k+1} = \left\{\gamma + 2\delta \cos\left(\frac{2\pi j}{N}\right)\right\} \phi_j^k \\ &= \frac{2}{(\beta_N \hbar)^2} \left\{1 - \cos\left(\frac{2\pi j}{N}\right)\right\} \phi_j^k = \frac{4}{(\beta_N \hbar)^2} \sin^2\left(\frac{\pi j}{N}\right) \phi_j^k \end{aligned}$$

and therefore for the overall vector  $\phi_j$ :

$$\begin{aligned} \mathbf{A}\phi_j &= \omega_j^2 \phi_j \\ \omega_j &= \frac{2}{\beta_N \hbar} \sin\left(\frac{\pi j}{N}\right) \end{aligned}$$

The eigenfunctions for the original boundary condition  $y_1 = y_{N+1} = 0$  can be obtained by only considering the imaginary part of  $\phi_j$ . This operation has no impact on the eigenvalues obtained above whatsoever and therefore the  $\omega_j$  also depict the eigenfrequencies of the original problem.

The matrix  $\mathbf{A}$  can be easily expanded by adding  $\omega^2 \mathbb{I}$ , where  $\mathbb{I}$  depicts the  $N \times N$ -dimensional identity matrix, to yield the matrix representation  $\tilde{\mathbf{A}}$  of the operator  $\left\{-\frac{d^2}{dt^2} + \omega^2\right\}$ .  $\phi_1 \dots \phi_N$  still forms the eigenbasis of  $\tilde{\mathbf{A}}$  and the eigenvalues are given by

$$\begin{aligned} \tilde{\mathbf{A}}\phi_j &= (\omega_j^2 + \omega^2) \phi_j \\ \omega_j &= \frac{2}{\beta_N \hbar} \sin\left(\frac{\pi j}{N}\right) \end{aligned} \tag{18}$$

Thus equation (18) is the finite dimensional approximation to equation (12) and yields the latter if the limit  $N \rightarrow \infty$  is carried out. To see this it is convenient to fix an arbitrary eigenfrequency  $\omega_i$  first and then consider the impact of  $N \rightarrow \infty$  on this particular eigenfrequency. For  $i$  arbitrary but fixed it follows from Taylor's Theorem that  $\sin\left(\frac{\pi i}{N}\right) \rightarrow \left(\frac{\pi i}{N}\right)$  if  $N \rightarrow \infty$  ( $\frac{i}{N} \ll 1$  because  $i$  is fixed and  $N \rightarrow \infty$ ). Therefore

$$\omega_i = \frac{2}{\beta_N \hbar} \sin\left(\frac{\pi i}{N}\right) \xrightarrow{N \rightarrow \infty} \frac{2N}{\beta \hbar} \left(\frac{\pi i}{N}\right) = \frac{2\pi i}{\beta \hbar}$$

This is just the eigenfrequency that occurs in formula (12). Since formula (12) is really only valid for continuous functions (which is equivalent to the limit  $N \rightarrow \infty$ ) it is crucial to use the  $\omega_i$  of (18) in the finite dimensional formula (17).

## 2.4 Multidimensional Generalisation

Paths, as already mentioned above, are essentially one dimensional objects whatever the dimension of the space they are defined on might be. Since the derivation of formula (15) essentially only depends on an integration over paths, which is essentially one dimensional as well, the formula for the tunnelling splitting generalises in a straight forward way to more dimensions. Of course one has to take into account that positions  $\vec{x}$  and momenta  $\vec{p}$  are now given by vectors and also the path integral measure  $\mathcal{D}x$  becomes a multidimensional  $\mathcal{D}\vec{x}$  (this can be thought of:  $\mathcal{D}\vec{x} = \mathcal{D}x^1 \mathcal{D}x^2 \dots \mathcal{D}x^f$  for a  $f$ -dimensional system). Although this does not alter equation (15), it does lead to some changes in the finite dimensional approach. To illustrate this, a  $f$ -dimensional Hamiltonian of the form  $H = \sum_{j=1}^f \frac{1}{2} m^j (\dot{x}^j)^2 + V(x^1, \dots, x^f)$  for a particle with mass  $m = (m^1, \dots, m^f)$  and position  $\vec{x} = (x^1, \dots, x^f)$  is considered. The finite dimensional approach therefore yields:

$$\begin{aligned} H[x_i] &= V(x_i^1, \dots, x_i^f) + \sum_{j=1}^f \frac{m^j}{2 \left(\hbar \frac{\beta}{N}\right)^2} \left(x_{i+1}^j - x_i^j\right)^2 \\ S_{ins} &= \int_0^{\hbar\beta} H[\vec{x}_{ins}(\tau)] d\tau \approx \frac{\hbar\beta}{N} \sum_{i=1}^N H[x_i] \\ S_0 &= \frac{N}{\hbar\beta} \sum_{i=1}^N \sum_{j=1}^f \left(x_{i+1}^j - x_i^j\right)^2 \end{aligned}$$

Therefore the one dimensional definitions for the instanton trajectory  $\tilde{x}$  from above have to be altered.

$$\begin{aligned}
\beta_N &:= \frac{\beta}{N} \\
\tilde{U}_N &:= \sum_{i=1}^N \left( V(\tilde{x}_i^1, \dots, \tilde{x}_i^f) + \sum_{j=1}^f \frac{m^j}{2(\hbar\beta_N)^2} (\tilde{x}_{i+1}^j - \tilde{x}_i^j)^2 \right) \\
B_N &:= \sum_{i=1}^N \sum_{j=1}^f (\tilde{x}_{i+1}^j - \tilde{x}_i^j)^2 \\
g &:= \left( \prod_{j=1}^f m^j \right)^{\frac{1}{f}}
\end{aligned}$$

Only two changes in formula (17) occur. One is that the mass  $m$  is replaced by the averaged mass  $g$ . Furthermore the harmonic approximation to an  $f$ -dimensional potential is given by  $V(x^1, \dots, x^f) \approx \sum_{j=1}^f \frac{1}{2} m^j (\omega^j)^2 (x^j)^2$ , so not only one single frequency  $\omega$  but rather  $f$  different  $\omega^j$  (one for each dimension) have to be considered in the calculation of  $Q_0$ . This leads to the multidimensional generalisation of formula (17)

$$\frac{\Delta}{2} = \frac{1}{\beta_N \hbar} \left( \frac{g B_N \prod_{i=1}^N \prod_{j=1}^f \beta_N \hbar \sqrt{(\omega_i^j)^2 + (\omega^j)^2}}{4\pi \beta_N \prod_{i=1}^{Nf} \beta_N \hbar \sqrt{\eta_i}} \right)^{\frac{1}{2}} e^{-\frac{1}{2} \beta_N \tilde{U}_N} \quad (19)$$

**Comment:** In principal the treated curves do not need to lie in  $\mathbb{R}^n$ , but could also be restricted to some arbitrary manifold  $M$ . This is possible, because paths on manifolds are again still one dimensional objects. It is therefore possible to generalise the formula for the tunnelling splitting in a way, such that it is also valid for restrained systems. Thus special boundary conditions (like total angular momentum conservation) could be fulfilled automatically by restraining the system to movements in space which fulfil these conditions automatically. But since restraining the movement of the system from  $\mathbb{R}^n$  to a submanifold of  $\mathbb{R}^n$  changes the metric in a nontrivial way (the scalar product becomes position-dependent), this generalisation is rather challenging and would go beyond the scope of this thesis.

## 2.5 RPMD-Theory and the Numerical Algorithm

To apply formulas (17) and (19) it is essential to know the classical trajectory  $x_{ins}$  which always exists but which can only rarely be calculated analytically. Therefore numerical methods have to be developed to approximate  $x_{inst}$ . One such approach is given by RPMD-theory (**R**ing **P**olymer **M**olecular **D**ynamics)

[5, 10, 4]. This theory makes clever use of the finite dimensional approximation of  $S[x(t)]$  and shall be explained for a one dimensional system. The generalisation to more dimensions is straightforward and can be done in the same way as explained above.

$$S[x(\tau)] \approx \hbar\beta_N U_N(x_1, \dots, x_N) \quad (20)$$

$$U_N(x_1, \dots, x_N) := \sum_{i=1}^N \left( V(x_i) + \frac{1}{2}m\omega^2(x_{i+1} - x_i)^2 \right) \quad (21)$$

with  $\omega := \frac{1}{\beta_N \hbar}$  and periodic boundary conditions ( $x_{N+1} = x_1$ ). As already described in (16) (where formula (20) was already used to approximate  $x_{ins}$ ),  $x_k$  describes the position of the system following the path  $x$  in configuration space after imaginary time  $\tau_k = k\frac{\beta\hbar}{N}$ . Using the notation  $\omega = \frac{1}{\beta_N \hbar}$  it can clearly be seen that  $U_N(x_1, \dots, x_N)$  is in fact nothing but the potential energy of a classical ring polymer (a closed {because  $x_{N+1} = x_1$ } chain of point masses that are connected by harmonic springs with frequency  $\omega := \frac{1}{\beta_N \hbar}$ . All point masses have the actual physical mass  $m$  of the considered system) that is affected by an external potential  $V(x)$ .

The desired instanton trajectory  $x_{ins}$  corresponds to a saddle point of the action functional  $S_E[x]$ . Thus a numerical approximation to  $x_{ins}$  can be obtained by finding a saddle point of the fictitious PES  $U_N(x_1, \dots, x_N)$ . Every saddle point of a PES corresponds to a vanishing force  $\vec{F} = -\nabla U_N$  which means in this case

$$-\nabla U_N = -\sum_{i=1}^N \left( V'(x_i) + \frac{m}{(\beta\hbar)^2} (x_{i+1} - 2x_i + x_{i-1}) \right) = 0$$

However this is nothing but a finite dimensional approximation to the Euler Lagrange equation for the Euclidian action which can be seen if the whole expression is multiplied by  $\frac{\beta\hbar}{N}$ .

$$\begin{aligned} -\frac{\beta\hbar}{N} \nabla U_N &= -\frac{\beta\hbar}{N} \sum_{i=1}^N \left\{ V'(x_i) + \frac{m}{\beta\hbar} \frac{(x_{i+1} - x_i) - (x_i - x_{i-1})}{\beta\hbar} \right\} \\ &\approx -\frac{\beta\hbar}{N} \sum_{i=1}^N \left\{ V'(x_i) + m \frac{\dot{x}_{i+1} - \dot{x}_i}{\beta\hbar} \right\} \approx -\frac{\beta\hbar}{N} \sum_{i=1}^N \left\{ V'(x_i) + m\ddot{x} \right\} \\ &\approx -\int_0^{\hbar\beta} \left\{ V'(x_i) + m\ddot{x} \right\} dx = 0 \end{aligned}$$

This again shows what a close connection exists between RPMD (and thus classical mechanics) and the instanton theory.

With RPMD theory the crucial problem of finding a numerical approximation to  $x_{ins}$  can be converted into the problem of finding a non trivial saddle point (transition state) of the fictitious PES  $U_N$ . This problem is already very well known and established in theoretical chemistry (e.g. transition state theory). Thus

various methods and algorithms have already been published for this purpose. The algorithm used for this thesis was developed by Nichols and co-workers [11] and works stepwise. At each step the local gradient  $\vec{F}$  and the local Hessian  $H$  are used to compute a step vector  $\vec{x}$  which leads to new coordinates where this process can be repeated. In order to approach a saddle point, the step vector  $\vec{x}$  is chosen to yield negative first order and total energy changes along all but one (the lowest) eigenmode of  $H$  (for approaching a minimum the energy changes would be chosen to be negative along all eigenmodes). This means “moving” uphill along the lowest Hessian eigenmode while remaining at minima along the other eigenmodes. Doing so creates a “steam-bed” walk along the lowest eigenmode that leads to the desired transition state.

## 2.6 Validity of the approximations

Formula (19) was derived within the frame of rigorous theoretical physics by making the use of only two approximations: the harmonic approximation to the path integral formalism, finite dimensional approximations to the derivative ( $\frac{d}{dx}f(x) \approx \frac{f(x+h)-f(x)}{h}$ ), the integral ( $\int_a^b f(x) dx \approx \frac{b-a}{N} \sum_{i=1}^N f(x_i)$ ) and to the eigenvalues of a particle in a box, as well as a Taylor expansion of  $\cosh(\beta \frac{\Delta}{2}) = 1 + \frac{1}{2!} (\beta \frac{\Delta}{2})^2 + \mathcal{O}(\beta^4)$ . Richard Feynman proposed in [9] that the harmonic approximation yields very good results as soon as the ratio of action  $S$  and  $\hbar$  (recall that  $\frac{S_{\text{ins}}}{\hbar} = \beta_N \tilde{U}_N$ ) along the classical trajectory exceeds 1. Due to the masses and velocities involved, this condition is essentially always fulfilled in tunnelling processes relevant for chemistry (e.g.: for malonaldehyde:  $\beta_N \tilde{U}_N > 3$  as it can be seen in section 3.2, Table 1). Finite dimensional approximations of derivatives and integrals resemble the (Riemannian) definitions of these objects and are known to yield good results if the step size is sufficiently small (i.e. if  $N$  is sufficiently large). The finite dimensional approximation to the eigenvalues of a particle in a box resembles a discrete fourier transform (DFT) approximation to the continuous fourier transform (FT). It is well known that the DFT approximation is valid as soon as its dimensionality is reasonably large.

Therefore all approximations that were used in this section are either well established numerical approaches to mathematical entities (integral, derivative, FT) or a sufficient condition is known (harmonic approximation) which, if met, guarantees the validity of the approximation.

## 3 Applications

Testing and applying formulas (17) and (19) to different systems was the main purpose of this research project. Throughout this thesis the whole programming work was done in python. A numerical algorithm implemented by Jeremy O. Richardson, based on the RPMD theory and the Nichols-algorithm [11] explained above, was used to obtain numerical approximations for the instanton

trajectory  $x_{inst}$ .

### 3.1 The One-dimensional Double Well

Since Formula (17) is finite dimensional it is far more relevant for actual computation than formula (15). In this section formula (17) is applied to a particle in a simple one dimensional double well potential

$$V(x) = \lambda(x^2 - x_0^2)^2 \quad x_0, \lambda \in \mathbb{R}, \lambda > 0$$

The big advantage of this system is that the tunnelling splitting can be computed relatively easily in three different ways. Thus the double well potential provides an ideal opportunity to test the results obtained above in a purely computational way. Before the actual results are discussed, the alternative approaches are introduced and briefly discussed.

#### 3.1.1 Instanton Approach

The core of this method is formula (17). To apply this formula it is crucial to know  $x_{inst} = x_{inst}(\hbar\beta)$  for a sufficiently large  $\beta$  (as discussed above, formula (15) is only exact in the  $\lim \beta \rightarrow \infty$ ). Formally  $x_{inst} : \tau \rightarrow \mathbb{R}$  is  $C^1$  with  $\tau \in [0, \hbar\beta]$ . In the numerical approximation of  $x_{inst}$  the interval  $[0, \hbar\beta]$  is sliced into a number of  $N$  finite dimensional (imaginary) time steps. If  $\beta$  is increased, the total length of the interval becomes bigger and therefore more time steps are required to give an accurate approximation. Obtaining a decent trajectory  $x_{inst}$  for high  $\beta$  therefore requires an increase of  $N$  as well, as it can be seen in figures 4 and 5.

#### 3.1.2 Accurate Quantum Mechanical Treatment

Since the potential  $V(x) = \lambda(x^2 - x_0^2)^2$  does not depend explicitly on time, the one dimensional Hamilton operator  $\hat{H} = \frac{p^2}{2m} + V(x)$  is time-independent and the Schroedinger equation

$$i\hbar \frac{\partial}{\partial t} \Psi = \hat{H} \Psi \quad (22)$$

is therefore separable. Thus the solutions of equation (22) are stationary ones and can be obtained by solving the time independent Schroedinger equation

$$\hat{H} \Psi = E \Psi \quad (23)$$

Since the tunnelling splitting factor  $\Delta$  is nothing but the energy difference between the two lowest eigenstates, it can be obtained by finding and subtracting the two lowest eigenvalues  $E_0$  and  $E_1$  of equation (23). It is well established, that eigenfunctions and eigenvalues of a linear operator  $\hat{A}$  can be obtained by diagonalising its matrix representation

$$\hat{\mathbf{A}}_{ij} = \langle \phi_i | \hat{A} | \phi_j \rangle$$

different instantons

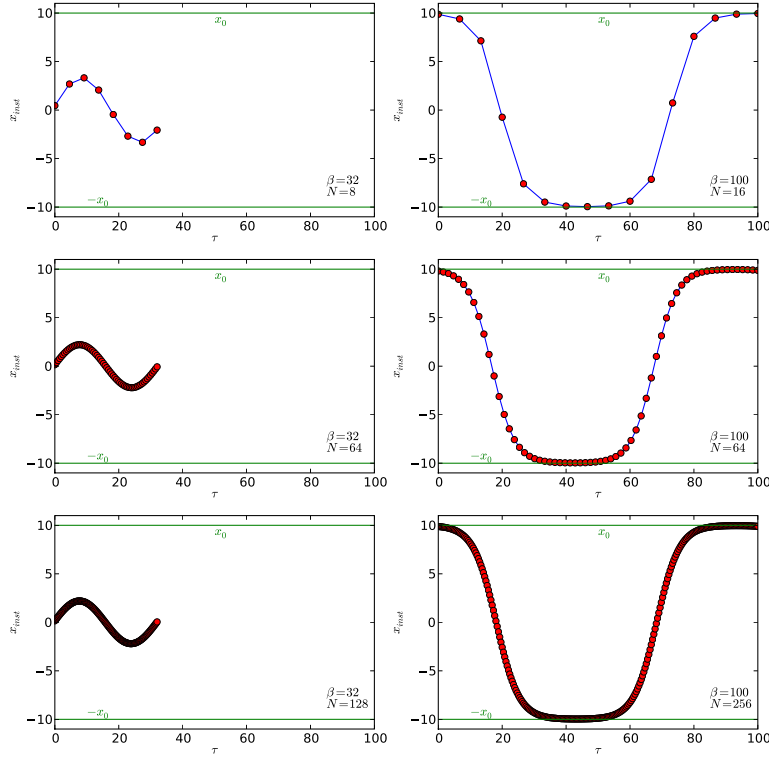


Figure 4: Finite dimensional instanton approach for a double well potential with  $x_0 = 10$  and  $\lambda = 10^{-4}$ .

In the left column the finite dimensional approach to  $x_{inst}$  is shown for  $\beta = 32$  (just above  $\beta_{cross}$  which is 31.5 for this geometry) and different numbers of time steps  $N$ . The trajectory doesn't reach the minimum positions  $-x_0$  and  $x_0$  (green lines) at all which shows that the finite dimensional approach to  $x_{inst}$  is insufficient if  $\beta$  is not big enough.

The right column shows the approach for  $\beta = 100$  and different  $N$ . Here the approach to  $x_{inst}$  is far better and it can be seen very clearly that a higher number of beads  $n$  is required to give an accurate approximation to the actual instanton trajectory.

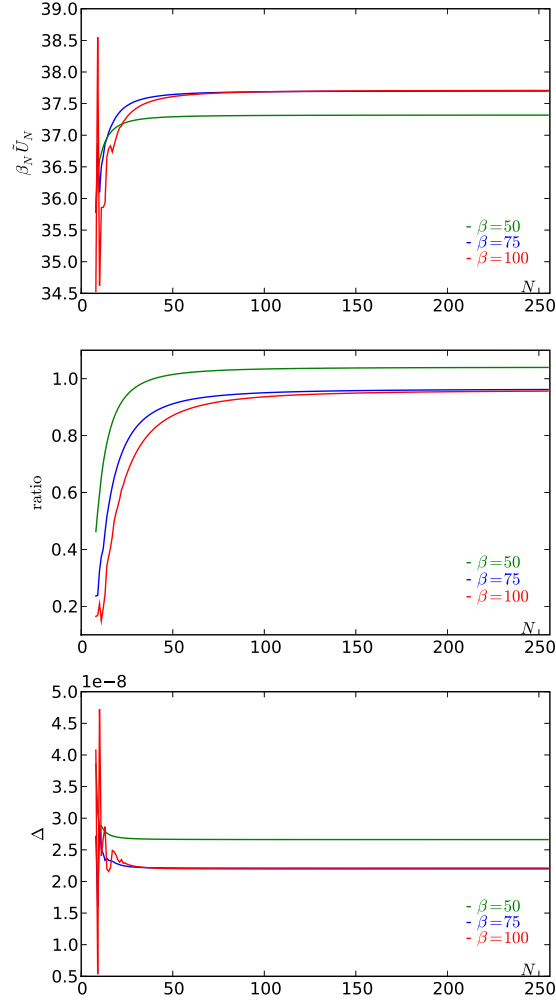


Figure 5: Convergence of the important parts of formula (17) for different  $\beta$  with respect to the number of time steps  $N$  for a double well potential with  $x_0 = 10$  and  $\lambda = 10^{-4}$  ( $\beta_{cross} = 31.5$ ). Here ratio stands for  $\prod_{i=1}^N \sqrt{\omega_i^2 + \omega^2} \left( \prod_{i=3}^N \sqrt{\eta_i} \right)^{-1}$ .

It can again be seen clearly that in all three cases the convergence becomes slower as  $\beta$  is increased. But as figure 4 shows, it is nevertheless necessary to pick a sufficiently large  $\beta$  to obtain accurate results.

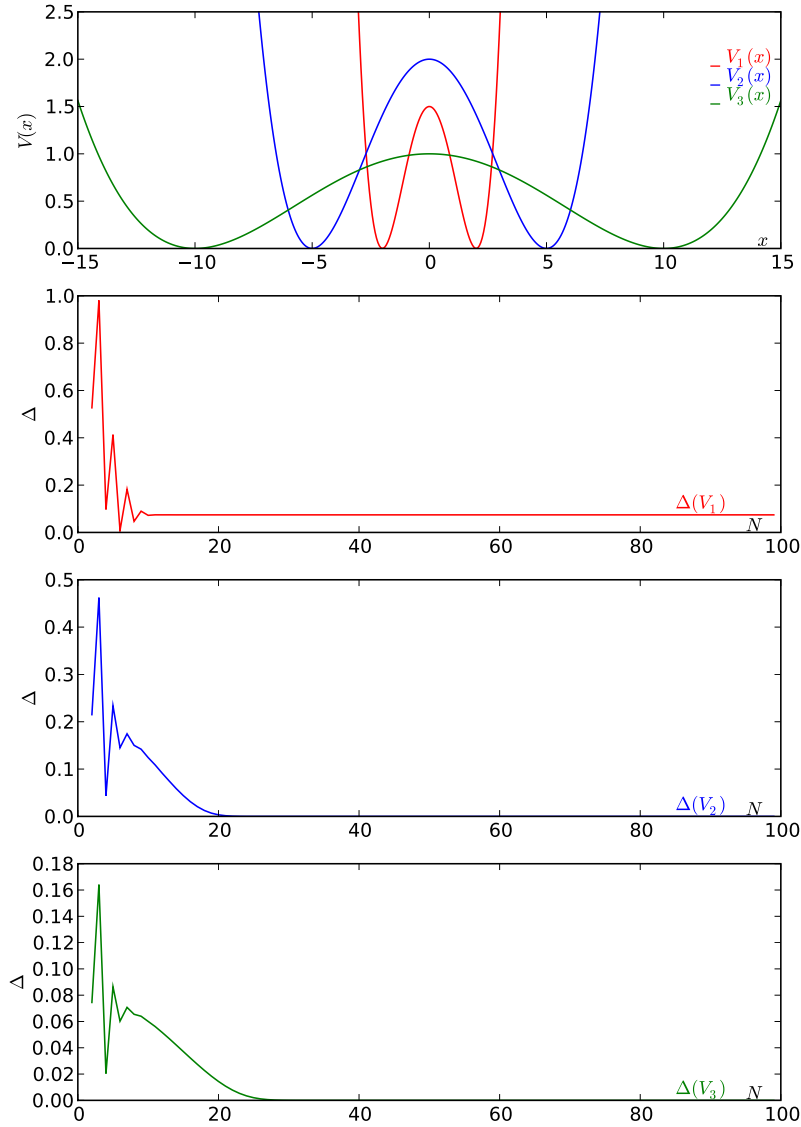


Figure 6: Convergence of the factor  $\Delta$ . Here the tunnelling splitting  $\Delta$  is obtained by diagonalising the  $N \times N$ -matrix representation  $\hat{\mathbf{H}}_{ij}$  of the Hamilton operator  $\hat{H}$ . In this figure  $\Delta = \Delta(N)$  is depicted with respect to the dimensionality  $N$  of the matrix. The results are shown for three different double well potentials  $V_1(x)$   $\{x_0 = 2, \lambda = \frac{3}{32}\}$ ,  $V_2(x)$   $\{x_0 = 5, \lambda = \frac{2}{625}\}$  and  $V_3(x)$   $\{x_0 = 10, \lambda = \frac{1}{10^4}\}$ .

where  $\{\phi_i\}_{i \in \mathbb{N}}$  is an arbitrary orthonormal basis set of the considered Hilbert space  $\mathcal{H}$  and  $\langle \phi_i | \hat{A} | \phi_j \rangle = \langle \phi_i, \hat{A} \phi_j \rangle$ , where  $\langle , \rangle$  denotes the scalar product induced by  $\mathcal{H}$ . For the purpose of obtaining the tunnelling splitting factor  $\Delta$  numerically, a python code was written that approximates  $\Delta$  by diagonalising “big” matrix representations of the above Hamiltonian and comparing the lowest two eigenvalues. This algorithm only yields exact results in the limit  $N \rightarrow \infty$ , where  $N$  denotes the dimension of the matrix representation ( $\hat{\mathbf{H}}_{ij} \in M_{N \times N}$ ). But as figure 6 shows, the obtained value of  $\Delta$  converges rather quickly. As basis functions harmonic oscillator eigenfunctions have been chosen which turned out to be a rather clever choice, because - due to the recursion relation of Hermite polynomials - the  $\hat{\mathbf{H}}_{ij}$  can all be calculated analytically and that greatly speeds up the program.

### 3.1.3 Analytical Semiclassical Result

Instead of depicting the saddle point solution of  $\frac{\delta S[x]}{\delta x} = 0$  in terms of the instanton (a periodic trajectory in the upside down potential), one can describe the saddle point trajectory with kinks (movement from the first minimum to the second minimum) and antikinks (the opposite movement). By doing so the whole problem can be solved analytically for this particular potential in the limit  $\beta \rightarrow \infty$ , as Benderskii [8] shows. This calculation yields the analytical semiclassical formula

$$\begin{aligned} \Delta &= \frac{\omega_0}{\pi} \left( 2\pi \frac{\omega_0^3}{\lambda} \right)^{\frac{1}{2}} \exp \left\{ -\frac{\omega_0^3}{12\lambda} \right\} \\ \omega_0 &= \sqrt{\frac{8\lambda x_0^2}{m}} \end{aligned} \quad (24)$$

Being able to solve the problem exactly happens very rarely and is in general only possible for very easy systems. This restricts the analytical method to simple systems and approximate approaches (like the methods introduced in section 1) have to be used for more complex ones. Being able to compare the results of the approximate RPMD-instanton approach with the analytical semiclassical result however is a big advantage of this double-well potential.

### 3.1.4 Results and Discussion

To test the validity of formula (17) python codes were written to evaluate the results of the three different approaches. These algorithms were applied to various different double well potentials to investigate their dependence on properties of the PES like the barrier height and barrier width. The results for three different potential surfaces are listed in the following table. Figure 7 shows these different PESes. Since this application is purely computational, the collective energy unit for  $V_i(x)$  and  $\Delta$  can be chosen completely arbitrarily.

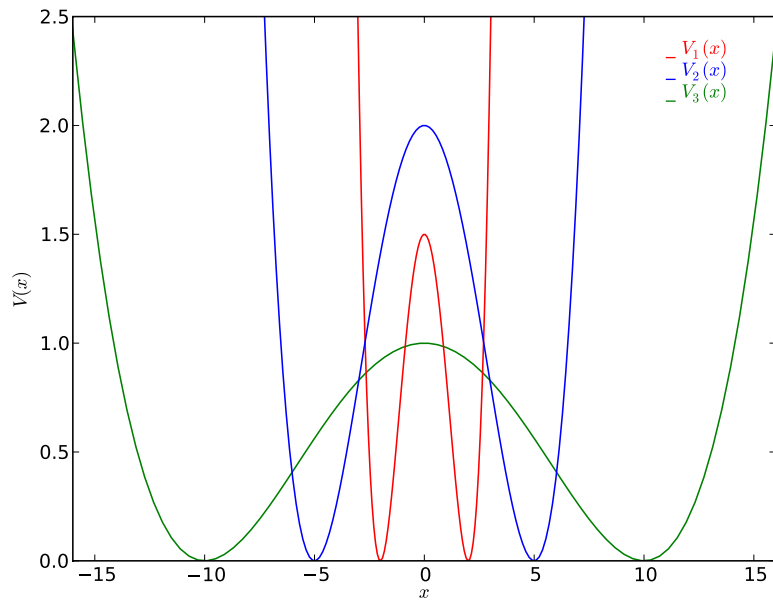


Figure 7: Plot of the three different potential surfaces that lead to the results listed in the table. In comparison  $V_1$  has the narrowest,  $V_2$  the highest and  $V_3$  the widest barrier region.

$V(x_0, \lambda, \beta_{cross})$	$\Delta_{\hat{H}_{ij}}$	$\Delta_{\text{kink}}$	$\Delta_{\text{instanton}}$
$V_1(2, \frac{3}{32}, 5.13)$	0.0742	0, 1015	0.1012 ( $\beta = 20$ )
$V_2(5, \frac{2}{625}, 11.1)$	$1.2056 \times 10^{-5}$	$1.3077 \times 10^{-5}$	$1.3067 \times 10^{-5}$ ( $\beta = 40$ )
$V_3(10, \frac{1}{10^4}, 31.42)$	$2.0771 \times 10^{-8}$	$2.1962 \times 10^{-8}$	$2.1967 \times 10^{-8}$ ( $\beta = 100$ )

Obviously both semiclassical results  $\Delta_{\text{kink}}$  and  $\Delta_{\text{instanton}}$  deviate from the actual quantum mechanical result  $\Delta_{\hat{H}_{ij}}$ . The approximate result  $\Delta_{\text{instanton}}$  reproduces the exact semiclassical result  $\Delta_{\text{kink}}$  in a very encouraging way. However it seems that formula (17) provides the best results for barriers that are not too small and narrow (see figure 7). This is because perturbation theory was used to obtain the energies in equation (1) and this theory only yields good results for relatively small perturbations. In this case the perturbation is given by the interference of the two wave functions of the different wells. This interaction is only possible due to the tunnelling effect and therefore becomes smaller if the height and width of the barrier increases. Thus a small perturbation corresponds directly to a rather big and wide barrier.

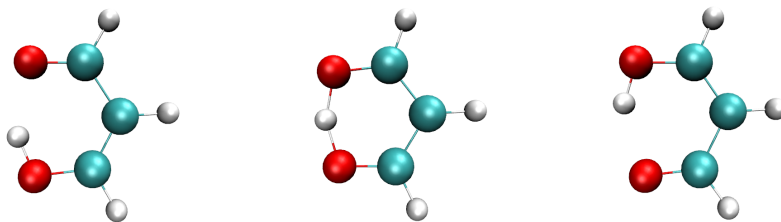


Figure 8: First equilibrium, transition state and second equilibrium for the tunnelling process in malonaldehyde. It can be clearly seen that the two equilibrium states are equivalent since they can be converted into each other by a rotation.

### 3.2 The tunnelling splitting in malonaldehyde

Malonaldehyde (MA) is one prime example for multidimensional tunnelling. It yields an extraordinary high value for the tunnelling splitting and is an already very well studied system. Accurate experimental values for the tunnelling splitting ( $\Delta = 21.6 \text{ cm}^{-1}$ ) based on far-infrared spectroscopic data [3] and various theoretical treatments [12, 13, 14] have already been published. The possibility of comparing the results from formula (19) for this system with other theoretical approaches and accurate experimental results makes MA a valuable benchmark for the theory developed above.

#### 3.2.1 The considered Potential Energy Surface

Since the equilibrium geometry and the transition state of the molecule are both planar, the out of plane motion can be expected to have little impact on the tunnelling. For this reason a potential surface was chosen that neglects out-of-plane movement. This reduces the dimensionality of the problem from 21 dimensions (3D:  $f = 3N - 6$ , where  $f$  denotes the number of degrees of freedom and  $N$  the number of atoms) to 15 dimensions (2D:  $f = 2N - 3$ ). For the actual calculation a potential published by Guo and co-workers [13] was used. Unfortunately this potential turned out to be not very accurate. Guo's potential yields a barrier height of roughly  $3500 \text{ cm}^{-1}$  but newer experiments [3] have shown that the actual height is about  $2000 \text{ cm}^{-1}$ . Thus the tunnelling splitting obtained by using this PES must be expected to be lower than the experimental value because a far higher barrier is assumed.

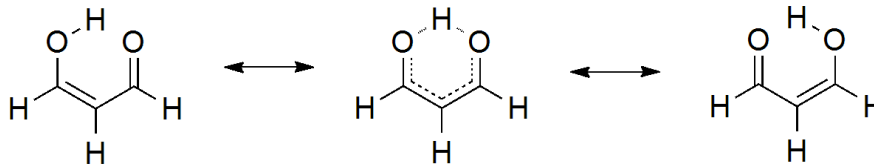


Figure 9: Chemical structure of the equilibrium geometries (left and right) and the transition state (middle) of malonaldehyde

### 3.2.2 Computational Details

In order to obtain a value for the tunnelling splitting  $\Delta$  formula (19) was applied to the 18 dimensional Cartesian PES of MA. In order to do so Guo's potential surface, that was given in internal coordinates, was transformed into Cartesian coordinates and digitalised. Additional expenditure was accepted to calculate the resulting force analytically in Cartesian coordinates. This was worthwhile because knowing the force analytically speeds up the algorithm that approximates  $x_{ins}$  numerically. Python codes were written that calculated all parameters  $(U_N, \eta_i, \omega_i)$  necessary for formula (19) from the instanton trajectory. Finally a code for formula (19), that was again implemented by Jeremy O. Richardson, was used to obtain the desired tunnelling splitting  $\Delta$ .

### 3.2.3 Results

It is well known that tunnelling effects depend strongly on the mass of the involved particle [2, 7]. Thus the isotopic effect on  $\Delta$  is expected to be rather big. In order to explore the impact of the isotopic effect the tunnelling splitting  $\Delta$  was calculated for a malonaldehyde molecule with a normal hydrogen atom as tunnelling particle (H-MA) and a malonaldehyde isotope with a deuterium atom as tunnelling particle (D-MA). The crossover temperature for both systems was calculated to be  $\beta_{cross}^H = 0.67$  for H-MA and  $\beta_{cross}^D = 0.89$  for D-MA respectively. The actual calculations were performed at  $\beta^H = 15$  and  $\beta^D = 20$ . Results for different numbers of  $N$  are collected in Table 1.

### 3.2.4 Discussion

A rule of thumb, which is valid in the treatment of the double well and various other problems, states that for obtaining accurate instanton trajectories it is usually sufficient to set  $\beta \approx 3\beta_{cross}$ . The observed system however has the interesting property that this rule of thumb fails and an extraordinary large  $\beta$  ( $\beta \gtrsim 20\beta_{cross}$ ) is required. The bigger  $\beta$  gets, the longer it takes the algorithm

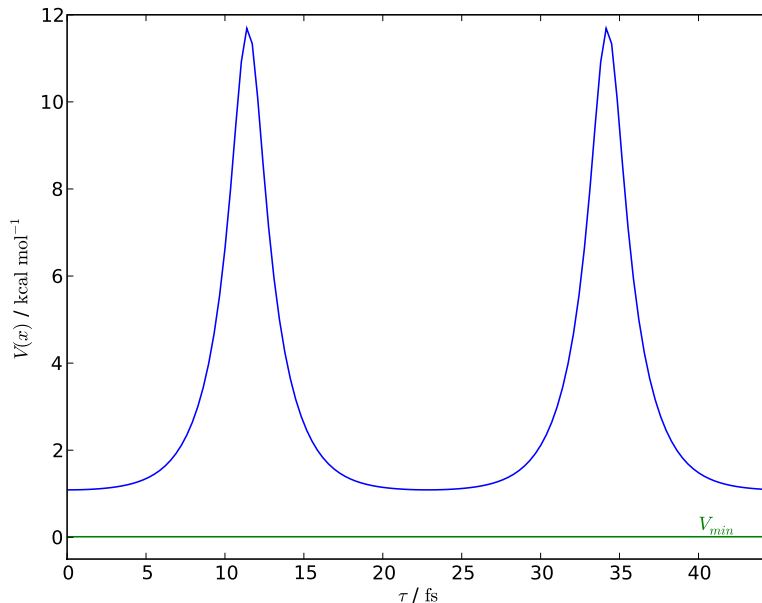


Figure 10: Plot of the approximate instanton trajectory  $x_{ins}$  of malonaldehyde against the potential  $V(x)$  for  $\beta = 3$ . This figure clearly depicts the typical properties of the instanton.  $x_{ins}$  stays a long time in the vicinity of the first potential minimum, crosses the barrier region (high potential) during some short time (first peak) to reach the second potential minimum. There it stays for another long time and recrosses the barrier region during some short time (second peak) again. It can be furthermore seen that  $x_{ins}$  has not properly converged yet because it does not reach the actual potential minimum  $V_{min}$ .

#### H-MA

$N$	$\beta_N \bar{U}_N$	$\sqrt{\text{ratio}}$	$\Delta$
8	3.986	0.454	33.88
16	7.313	0.694	12.81
32	11.095	3.822	11.31

#### D-MA

$N$	$\beta_N \bar{U}_N$	$\sqrt{\text{ratio}}$	$\Delta$
8	5.192	0.348	16.218
16	9.463	0.599	4.262
32	13.966	3.440	2.694

Table 1: Numerical results for different numbers of  $N$  at  $\beta^H = 15$  and  $\beta^D = 20$ , where  $\text{ratio} := \prod_{i=1}^{Nf} \sqrt{\omega_i^2 + \omega^2} \left( \prod_{i=3}^{Nf} \sqrt{\eta_i} \right)^{-1}$ . The results differ from the experimental value  $\Delta = 21.6 \text{ cm}^{-1}$  for H-MA .

to converge and yield proper results for the instanton trajectory. Due to this and the high dimensionality of the system, finding an accurate instanton trajectory is time consuming. Limited time is therefore the reason why the table above is incomplete. It can be clearly seen that the values for the tunneling splitting  $\Delta$  have not converged yet. Calculations for higher  $\beta$  are currently carried out by Jeremy O. Richardson and I am positive that they will yield good results. It can however already be seen in this table that the obtained  $\Delta$  is smaller than the experimental value ( $\Delta = 21.6 \text{ cm}^{-1}$  for the H-MA). This is due to the inaccurate PES which assumes a barrier that is far too high, as already mentioned above. The isotopic effect however seems far more promising. The tunneling splitting parameter  $\Delta$  for  $N = 32$  is for the Hydrogen-Malonaldehyde is about 4 times bigger than the one for the molecule with Deuterium as a tunneling particle. This is close to theoretical predictions and experimental measurements that both predict a ratio of about 6.

## 4 Conclusion

In this thesis an approach for calculating the tunnelling splitting  $\Delta$  using RPMD-theory has been presented and applied to two benchmark examples - the one dimensional double well and malonaldehyde. By doing so the advantages and disadvantages of this approach became apparent and shall be briefly recapitulated here. Its main advantages are the theoretical independence of dimension and the physical rigour in derivation. Unlike many other methods [8], the RPMD-formalism does not need to assume effective one-dimensionality in a multidimensional problem, but generalises naturally to arbitrary dimensions. Furthermore the formula for  $\Delta$  was derived within the frame of rigorous theoretical physics by making use of only a few approximations that were discussed in Section 2.6. These approximations either follow from basic mathematics or, in the case of the harmonic approximation, sufficient conditions for their validity are known. It is therefore not necessary to introduce additional quantum mechanical concepts (such as density functionals) which makes the approach “neat” from a theoretical point of view. The validity of this formalism has been confirmed by its application to the one dimensional double well (section 3.1) where it resembled the actual quantum mechanical result very accurately.

The disadvantage of the approach turns out to be its computational expense. The process of approximating the instanton trajectory in a system of high dimensionality is a challenging computational problem and the “steam-bed”-algorithm is not yet a completely satisfactory solution. It became apparent in the treatment of malonaldehyde that this algorithm, while working well in low and moderate dimensions, becomes very slow for more complex problems which have a high dimensionality. Furthermore it turned out that increasing  $\beta$  worsens the convergence and destabilises the algorithm. This weakness is not conceptual but computational. Developing a better procedure for finding the saddle point of a high dimensional potential energy surface would diminish this disadvantage.

In the treatment of malonaldehyde another property of the RPMD-formalism became apparent: its dependence on the validity of the used PES. Knowledge about the energy surface flows into the approach via the potential energy dependence of the action  $S$  ( $S[x] = \int \left\{ \frac{m}{2} \dot{x}(t)^2 - V(x(t)) \right\} dt$ ). Therefore the whole concept requires exact knowledge of the potential energy surface and the challenging problem of finding an accurate PES remains to be solved. In the treatment of malonaldehyde it has been shown how crucial this dependence is. There a PES [13] was used which had been constructed using empirical data. Such a procedure naturally yields less accurate results than ab initio quantum chemistry methods. The author believes that the use of such an inaccurate energy surface (recall that in this PES the barrier height was furthermore assumed to be too low) is the reason why the obtained tunnelling splitting ( $\Delta = 6.861 \text{ cm}^{-1}$  for  $N = 64$ ) resembles the empirical value of  $\Delta = 21.4 \text{ cm}^{-1}$ [3] in a less accurate way than previous approaches. For comparison R. Meyer and T. Ha [14] obtained a value of  $\Delta = 22.0 \text{ cm}^{-1}$  by using a finite dimensional matrix approximation to a Hamiltonian describing the hydrogen transfer motion and the vibrations.

Despite the minor drawback of obtaining inaccurate results in the case of malonaldehyde, this thesis has shown that approximating tunnelling splittings via RPMD-theory is a sound idea. It would be very interesting to apply the presented formalism to tunnelling splittings in other systems. One particularly rapid system would be ammonia, since this molecule is the prime example for tunnelling splitting and very accurate potential energy surfaces are known.

**Acknowledgements** I would like to thank Jeremy O. Richardson for his precious advice and his dedicated guidance throughout this project.

## References

- [1] F. Hund, *Zur Deutung der Molekelspektren. III.*, ZS. f. Phys. **43**, 805 (1927)
- [2] R. P. Bell, *The Tunnel Effect in Chemistry* (Chapman & Hall, London, 1980).
- [3] D. W. Firth, K. Beyer, M. A. Dvorak, S.W Reeve, A. Grushov, K. R. Leopold, *Tunable far-infrared spectroscopy of malonaldehyde*, J. Chem. Phys. **94**, 1812 (1991)
- [4] I. R. Craig, D. E. Manolopoulos, *Quantum statistics and classical mechanics: Real time correlation functions from ring polymer molecular dynamics*, J. Chem. Phys. **121**, 3368 (2004).
- [5] J. O. Richardson, S. C. Althorpe, *Ring-polymer molecular dynamics rate-theory in the deep-tunneling regime: Connection with semiclassical instanton theory*, J.Chem.Phys **131**, 214106 (2009)
- [6] D. M. Dennison, G. E. Uhlenbeck, *The Two-Minima Problem and the Ammonia Molecule*, Phys. Rev. **41**, 313 (1932)
- [7] D. J. Wales, *Energy Landscapes* (Cambridge University Press, Cambridge, 2003)
- [8] V. A. Benderskii, D. E. Makarov and C. A. Wight, *Chemical dynamics at low temperatures* (Wiley, New York, 1994)
- [9] R. P. Feynman and A. R. Hibbs, *Quantum Mechanics and Path Integrals* (McGraw-Hill, New York, 1965)
- [10] D. Chandler, P. G. Wolynes, *Exploiting the isomorphism between quantum theory and classical statistical mechanics of polyatomic fluids*, J. Chem. Phys. **74**, 4078 (1981).
- [11] J. Nichols, H. Taylor, P. Schmidt, J. Simons, *Walking on potential energy surfaces*, J. Chem. Phys. **92**, 340 (1990)
- [12] G. V. Mil'nikov, *Practical implementation of the instanton theory for the ground state tunneling splitting*, J. Chem. Phys. **115**, 6881 (2001)
- [13] Y. Guo, T. D. Sewell, D. L. Thompson, *A full-dimensional semi-classical calculation of vibrational mode selectivity in the tunneling splitting in a planar model of malonaldehyde*, Chem. Phys. Lett. **224**, 470 (1994)
- [14] R. Meyer, T. Ha, *Quantum states of hydrogen transfer and vibration in malonaldehyde*, Molecular Physics **101**, 3263 (2003)